

Aging in short-ranged attractive colloids: A numerical study

G. Fof¹, E. Zaccarelli¹, S. Buldyrev², F. Sciortino¹ and P. Tartaglia¹

¹Dipartimento di Fisica and INFM Center for Statistical Mechanics and Complexity,
Universita di Roma "La Sapienza", Piazzale Aldo Moro 2, 00185 Roma, Italy

²Center for Polymer Studies and Department of Physics, Boston University, Boston, MA 02215, USA.

(Dated: April 14, 2024)

We study the aging dynamics in a model for dense simple liquids, in which particles interact through a hard-core repulsion complemented by a short-ranged attractive potential, of the kind found in colloidal suspensions. In this system, at large packing fractions, kinetically arrested disordered states can be created both on cooling (attractive glass) and on heating (repulsive glass). The possibility of having two distinct glasses, at the same packing fraction, with two different dynamics offers the unique possibility of comparing within the same model the differences in aging dynamics. We find that, while the aging dynamics of the repulsive glass is similar to the one observed in atomic and molecular systems, the aging dynamics of the attractive glass shows novel unexpected features.

PACS numbers: 64.70.Pf, 82.70.Dd

I. INTRODUCTION

In the last years, the physics of systems characterized by short-ranged attractive inter-particle interactions has been the focus of several investigations. A good example of this type of systems are colloidal solutions, since the intensity and the range of the potential can be finely controlled by changing the solvent properties or the chemistry of the dispersed particles. The short range of the attractive interaction produces thermodynamic features which are not observed in atomic or molecular systems (where the interaction range is always long ranged) [1, 2, 3, 4]. Recently, theoretical, numerical and experimental studies have focused on the dynamical properties of these systems. One of the most astonishing discovery is that, at high density, the metastable liquid is characterized by a non monotonic temperature dependence of the characteristic structural times: the dynamics slows down not only upon cooling (as commonly observed in molecular systems), but also upon heating. The slowing down upon heating can be so intense that a novel mechanism of arrest takes place at high T [5]. In the high density part of the phase diagram, for sufficiently short-ranged potentials, a re-entrant liquid-glass line is observed and a liquid phase emerges between two glasses. In other words, moving along a constant density path, it is possible to pass from a glass phase to a liquid phase and then again in a new glass phase just by progressively lowering the temperature. The two glasses are named "attractive glass" and "repulsive glass" due to the different mechanisms, respectively attraction and excluded volume, which control the dynamical slowing down [6]. In the re-entrant liquid region, between the attractive and repulsive glasses, dynamics is very unusual. Correlation functions show a subtle logarithmic decay, while the particle mean squared displacement follows a power-law in time.

The complex dynamics in short-ranged attractive systems has been interpreted within Mode Coupling Theory

(MCT) [7]. Theoretical predictions do not depend on the detailed shape of the attractive potential and have been confirmed for many different modelizations of the attractive tail. [8, 9, 10, 11, 12]. A set of simulations [13, 14, 15, 16] and experiments [17, 18, 19, 20, 21, 22] have confirmed the existence of such complex dynamics.

In numerical work based on the Square Well System (SWS), one of the simplest models studied, it has been shown that a diffusivity maximum in temperature appears when the width of the square well is short enough compared to the hard core diameter [15]. The calculation of the iso-diffusivity lines in equilibrium [14] confirms the reentrant behavior and the novel dynamics which take place in the reentrant region. Along an iso-diffusivity path, the decay of the density-density correlation functions, which at high temperature can be well described by a stretched exponential, becomes more and more uncommon upon cooling, showing at low T signs of logarithmic decay [13, 15, 23].

Previous numerical work has focused on equilibrium properties and on the dynamics near the predicted glass-glass transition [13, 14, 15, 24]. Here we report a study of the non-equilibrium dynamics. Starting from an equilibrium state in the re-entrant liquid region, the system is quenched both at low and high temperature. We are then able to explore within the same model the aging dynamics for the attractive and repulsive glass, to find out if the differences which characterize the dynamics in the glassy state show up also in the out-of-equilibrium evolution. We discover that, while the aging dynamics of the repulsive glass is similar to the one observed in atomic and molecular liquids [25, 26], the aging dynamics of the attractive glass shows novel unexpected features. We also report comparison with a recent experimental study of aging in short ranged colloidal systems [27]

II. SIMULATION DETAILS

We investigate a system that has been extensively studied earlier in the equilibrium regime, a binary square well mixture [15]. The binary system is a 50%-50% mixture of $N = 700$ particles. The two species (labeled A and B) are characterized by a diameter ratio $d_A = d_B = 1.2$. Masses are chosen to be equal and unitary. The attraction is modeled by a square well interaction defined according to:

$$V_{ij}(r) = \begin{cases} 0 & r_{ij} < d_{ij} \\ u_0 & d_{ij} \leq r_{ij} < d_{ij} + d_{ij} \\ 0 & r_{ij} \geq d_{ij} + d_{ij} \end{cases} \quad (1)$$

where $d_{ij} = (d_i + d_j)/2$, $i, j = A, B$ and d_{ij} has been chosen in such a way that $d_{ij} = (d_{ij} + d_{ij}) = 0.03$. We choose $k_B = 1$ and the depth of the potential $u_0 = 1$. Hence $T = 1$ corresponds to a thermal energy equal to the attractive well depth. The diameter of the small specie is chosen as unity of length, i.e. $d_B = 1$. Density is parametrized in terms of packing fraction $\phi = (d_A^3 N_A + d_B^3 N_B) / L^3 = 0.6$, where $i = N_i / L^3$, L being the box size and N_i the number of particles for each species. Time is measured in units of $\tau_B = (m_B / k_B)^{1/2}$. The unit has been chosen consistently with Ref. [15], where the same system has been studied in equilibrium. A standard MD algorithm has been implemented for particles interacting with SW-S potentials [28]. Between collisions, particles move along straight lines with constant velocities. When the distance between the particles becomes equal to the distance where $V(r)$ has a discontinuity, the velocities of the interacting particles instantaneously change. The algorithm calculates the shortest collision time in the system and propagate the trajectory from one collision to the next one. Calculations of the next collision time are optimized by dividing the system in small subsystems, so that collision times are computed only between particles in the neighboring subsystems.

With the present choice of parameters, the formation of crystallites during the simulation run is not observed. As compared to the monodisperse case, the slight asymmetry in the diameters allows us to follow the development of the slow dynamics over several orders of magnitude [14]. We choose to work at the packing fraction $\phi = 0.608$, being this density in the middle of the re-entrant region of the phase diagram, as shown in previous calculations [15]. At this density we prepared 60 independent configurations, equilibrated at the initial temperature $T_i = 0.6$. Subsequently we quenched these independent configurations to the desired final temperatures, and then we followed the evolution in time at constant temperature. The characteristic time of the thermostat has been chosen to be much smaller than the structural relaxation time and such that the system may equilibrate within one time unit. Each of the 60 independent configurations has been quenched to $T_f = 1.2$, i.e. in the repulsive glass, and to $T_f = 0.3$, i.e. in the attractive glass and run up to $t_f = 2 \times 10^4$. The numerical protocol is

illustrated in Fig. 1. Iso-density curves from Ref. [15] and the extrapolated ideal glass line from Ref. [23] are plotted together with the quench path selected in this work. Since the system, after the quench, is out of equilibrium, all averages represented in the text by the symbol $\langle \dots \rangle$ have been performed over the ensemble of the 60 initial independent configurations.

III. RESULTS AND DISCUSSION

Numerical investigations of aging in glassy materials are usually accomplished by rapidly quenching the system from an equilibrium state to a new state, where the characteristic time scale of the structural relaxation is much longer than the observation time. When the time scale of the final state exceeds the characteristic time of the simulation, equilibrium cannot be reached within the simulation time. Out of equilibrium time translation invariance does not hold and the state of the system does not only depend from the external parameters, but also from the time elapsed from the quench, the so-called waiting time t_w . Indeed in the aging regime other notable effects emerge, i.e. violation of the fluctuation-dissipation theorem [29, 30, 31, 32, 33] and strong dependence on the story of the system [25]. Thus, in out-of-equilibrium conditions correlation functions will depend both on the time of observation t and on the waiting time t_w , i.e. $C_A(t_w; t) = \langle A(t_w) A(t_w + t) \rangle$. Similarly, the one time properties (e.g. the static structure factor or the energy), will depend on the waiting time t_w .

The first quantity that we investigate is the average potential energy of the system U . At $t_w = 0^+$, i.e. instantaneously after the quenches to respectively $T_f = 1.2$ and $T_f = 0.3$, the two systems possess the same potential energy. Then, with t_w , they start evolving toward different energy values. The situation is represented in Fig. 2. While the system quenched to $T_f = 1.2$, i.e. in the repulsive regime, shows an increase in the potential energy (i.e. a progressive breaking of the interparticle bonding), the one quenched to $T_f = 0.3$ shows the opposite behavior. In both cases, the time dependence of the potential energy shows a fast short-time ($t_w < 1$) evolution (which reflects the equilibration of the fast degrees of freedom) followed by a much slower evolution, proper of the aging dynamics. The aging dynamics has detectable different trends at high and low temperatures. While at high temperatures a clear $\log(t_w)$ dependence of U is observed, at low T the time dependence in log scale is not linear and can be well fitted by $U = U_{eq} + t_w^{-\alpha}$, with $\alpha \approx 0.14$. A similar form was successfully adopted by Parisi for a binary system of soft spheres in the aging regime [30]. The time evolution of the aging structure can be followed by numerical calculation of the partial static structure factors, $S(q; t_w)$ defined as

$$S(q; t_w) = \langle \left(\sum_i e^{iq \cdot r_i(t_w)} \right)^2 \rangle / N \quad (2)$$

where the partial density variables are defined as $\rho_i(\mathbf{q}) = \frac{1}{N} \sum_{\mathbf{r}} \exp[i\mathbf{q} \cdot \mathbf{r}] \rho_i(\mathbf{r})$, and $n_i = N_i/N$ are the partial concentrations. In equilibrium, time translation invariance implies $S(\mathbf{q};t) = S(\mathbf{q};0)$, i.e. the static structure factor is a time independent function.

The inset of Fig. 3 shows $S_{AA}(\mathbf{q};t_w)$ for the quench to $T_f = 1.2$, for waiting times spanning 4 decades. Similarly to binary Lennard-Jones systems [25], the variation of the static structure factor is particularly small, for all components. With increasing t_w a very weak increase at all peaks of the structure factors is observed. This is shown in the main figure. Similarly for the $T_f = 0.3$ case, the $S(\mathbf{q};t_w)$ changes are very small. Interestingly enough, for the first peak (and only there) the trend is reverted with respect to the previous case, i.e. the intensity of $S_{AA}(\mathbf{q};t_w)$ around the peak decreases on aging. This observation agrees with equilibrium studies. Indeed, for the square well system, an increase in temperature produces an increase in the first peak toward the hard sphere limit whereas lowering the temperature only promotes the structure factor oscillations at large wave-vector [34]. It is perhaps interesting to recall that within MCT, the increase of S at the first peak is responsible for the formation of the repulsive glass, whereas the long lasting oscillations in the structure factor generates the kinetic arrest in the attractive glass [10].

Next we study the intermediate scattering function, i.e. dynamic density-density correlators. For a binary mixture this quantity is defined by:

$$\langle \rho_i(\mathbf{q};t) \rho_j(\mathbf{q};t^0) \rangle = S(\mathbf{q};t, t^0) \quad (3)$$

where the density variables $\rho_i(\mathbf{q};t)$ have been defined before. In equilibrium $\langle \rho_i(\mathbf{q};t) \rho_j(\mathbf{q};t^0) \rangle$ will depend only on the difference $t - t^0$. When the system ages the density-density correlators is a function of t_w and t . In this paper, we show $\langle \rho_i(\mathbf{q};t) \rho_j(\mathbf{q};t^0) \rangle$ as a function of t_w and the time difference $(t - t_w)$, i.e. $\langle \rho_i(\mathbf{q};t_w) \rho_j(\mathbf{q};t - t_w) \rangle$. The density correlation is normalized by $S(\mathbf{q};t_w)$. The upper panel of Fig. 5 shows the t_w dependence of $S_{AA}(\mathbf{q};t_w; t - t_w)$, with $q_B = 8.72$, which lies between the first and the second peak in the static structure factor. On increasing t_w , the decay of the correlation functions becomes slower and slower. The time needed to lose memory of the starting configuration grows. This is a typical feature of aging systems and it has been encountered both in experiments [27] and simulations [25]. The slowing down of the dynamics on increasing t_w resembles the way the structural arrest emerges in supercooled liquids on approaching the glass transition. Indeed, in this case, upon cooling two characteristic time scales emerge, a fast decay around a plateau value and a slow decay to zero. The time duration of the plateau becomes longer, the closer the system is to the glass transition. On the other hand, in the aging regime the control parameter is the waiting time t_w , which plays a role analogous to that played by T in equilibrium, i.e. the longer t_w the longer is the time requested to lose memory. In the same way as temperature measures the distance from the glass transition in

equilibrium liquids, t_w measures the progressive thermalization of the structural degrees of freedom. In summary, with increasing t_w the system develops a clear plateau, whose height is consistent with the value expected for the repulsive glass.

Similar results are shown in the lower panel of Fig. 5 for $q_B = 6.37$, which is close to the maximum of the static structure factor. Two main differences emerge between the correlators at the two wavevectors: (i) the relaxation time is longer for $q_B = 6.37$, (ii) the plateau is higher. Both these issues follow, as expected, the trend of the equilibrium results, where at the maximum of the structure factor a maximum of the relaxation time and of the non-ergodicity parameter is encountered [35].

The upper panel of Fig. 6 shows the density-density correlation functions for the quench at $T_f = 0.3$ for $q_B = 8.72$. Similarly to what we found in the previous case, the time of decay of the correlators grows with the waiting time t_w . However the shape of the functions is drastically different, confirming that even the aging dynamics reflects the differences noted in the previous equilibrium studies. Two notable differences with the $T_f = 1.2$ case are: (i) the strength of the relaxation (i.e. the height of the plateau) in aging is much more intense, being now close to one; (ii) the plateau does not significantly stretch in time (as shown in the inset) beyond $t - t_w \approx 1$. Similar trends are found for a q -vector closer to the first peak of the structure factor, as shown in the lower panel of Fig. 6.

A recent study of the glass-glass transition has suggested the possibility that the attractive glass is significantly destabilized by hopping processes [24], which in the present context can be associated with the breaking of the interparticle bonds. The data shown in the inset of Fig. 6 support such interpretation, since no clear plateau can be observed for $t_w > 1$.

A very interesting feature of the correlation functions in the aging regime is the property of scaling with waiting time. Theoretical studies suggest that correlators at different waiting time can be rescaled by the equation:

$$\langle \rho_i(\mathbf{q};t_w) \rho_j(\mathbf{q};t - t_w) \rangle = S(\mathbf{q};t_w) + \frac{h(t - t_w)}{h(t_w)} \quad (4)$$

where $S(\mathbf{q};t)$ accounts for the short time [36]. The $h(t) = t$ case is the so-called simple aging case. For a binary mixture of Lennard-Jones spheres the system follows (4) with $h(t) = t$ and $\alpha \approx 0.88$ [25].

We tried to apply this scaling relation to our system. We focus on the low temperature quench, since the high temperature one shows a phenomenology, which is similar to the Lennard-Jones case. In the case of aging of $T_f = 0.3$ no clear scaling of the correlation functions can be performed. In Fig. 7a we show the crude tentative of data scaling. Correlators have been shifted in time to superimpose the correlators in the region where $0.7 < q < 0.9$. Fig. 7b shows the same data, this time shifted to maximize superposition for $0.35 < q < 0.5$. In Fig. 8 the scaling coefficients t_c used to obtain the scaling in

Fig. 7 are shown as function of the waiting time t_w . It can be seen that even if they could be fitted with power laws (with an exponent 0.38 ± 0.1 different from the exponent found for the Lenard-Jones case), the collapse of the different t_w curves is not good.

It is worth to make a comparison of our numerical results with recent data measured by Pham et al [27], for a system of colloids with depletion interaction. In their experiment, they measure the density-density correlation function in the aging regime for two system at different polymer concentration, corresponding respectively to conditions where the repulsive and the attractive glass are expected. To better compare with Pham et. al data, we calculated the density dynamical structure factor (irrespective of the particle type) for the same q -vector of the cited experiment. Results are shown in Fig. 9 and Fig. 10 where the $T_f = 1.2$ and $T_f = 0.3$ quenches are respectively plotted together with the experimental results from Ref. [27] (lower panel). Slight differences in the plateau values can be ascribed to differences in the actual composition of the simulated (binary mixture) and experimental (slightly polydisperse system). The agreement between the numerical and the experimental data is impressive.

Another important two-time observable is the mean squared displacement (MSD). In aging, it is defined as $\langle |r(t + t_w) - r(t_w)|^2 \rangle$, where $r(t)$ is the position of the particle at time t and the average $\langle \cdot \rangle$ is performed over all the particles and the independent configurations. Here we focus on the total MSD, i.e. evaluated with no distinction between particles of the two species.

Fig. 11a shows the MSD for $T_f = 1.2$. In analogy with the case of the density correlators, at short times there is no significant t_w -dependence. At larger times the diffusive process is visible. When the waiting time becomes large, a plateau starts to emerge at intermediate times, between the ballistic (short time) and the diffusive (long time) regime. The duration of the plateau grows as t_w increases. As above, this behavior is similar to the one observed in previous simulations of a binary mixture of Lenard-Jones particles [25].

This three time-region behavior (ballistic, plateau, diffusive) is generally explained in terms of the so called cage effect. When repulsive interactions start to be dominant the system slows down since each particle starts to get trapped in a shell of first neighbor particles. The length of the plateau indicates the typical time that a particle needs to escape this cage. The value of the plateau stands at the typical size of a cage, i.e. around 10% of the diameter in agreement with Lindemann's melting criterion [37]. For $T_f = 0.3$, the MSD shows a completely different behaviour, (Fig. 11b). Its evolution can again be divided in three time-regions, but now the short time (ballistic) and the long time (diffusive) regions bracket a long intermediate region where the MSD appears to grow as a power-law in time, with an effective exponent which decreases with t_w . Differently from the previous case, no evident sign of a plateau is present, except for a

hint of a plateau at MSD = 0.001 which starts to develop for large waiting times for $t_w = 0.5$. This value is consistent with a displacement of the order of the width of the potential well, and can be interpreted as a result of particles bonding in the attractive well, i.e. as some sort of attractive cages. However, activated bond-breaking processes appear to destroy such a confinement on time scales longer than $t_w = 1$.

IV. CONCLUSIONS

In systems with short-ranged attractive potentials, an efficient competition between attraction and excluded volume generates a highly non trivial equilibrium dynamics and two kinetically distinct glasses. In the "attractive glass", the particle localization is controlled by the bonding distance, while in the "repulsive glass" localization is controlled by the neighbor location. This offers the unique possibility of studying two different aging dynamics within the same model. In this article, we have realized this numerically for a model system which shows both types of disordered arrested structures, the square well potential. We have found that the aging dynamics is clearly different for the two glasses, both in the waiting time evolution of the one-time quantities, and in the time evolution of the two-times quantities.

The results reported in this article refer to a simple model system which captures the essence of the physics introduced by the short-range attraction. The square well potential is indeed a satisfactory representation of the coarse-grained particle-particle potential in colloidal system, for example in the presence of depletion interactions. Of course, dynamical features of the solvent constituents and of the solvent-particle interactions may significantly affect the particle dynamics. In this respect, the experimental validation of the equilibrium results is very valuable.

In particular, we have shown that the partial static structure factor evolves with t_w , showing opposite trends in the two cases, i.e. the first peak grows with t_w for the repulsive glass while decreases for the attractive one. We have also shown that the decay of correlation functions becomes slower and slower on increasing t_w in both cases, but with noteworthy differences in the strength of the relaxation (much more intense for the attractive glass case) and in the shape of the relaxation itself. The analysis of the MSD brings clear evidence that, while in the repulsive case there is the emergence of a plateau, whose time duration increases significantly with t_w , in the attractive glass case this does not happen. Indeed, in short-ranged attractive colloids, activated processes can be associated with thermal fluctuations of order u , which allow particles to escape from the bonds. These processes generate a finite bond lifetime and, at the same time, may destabilize the attractive glass. It is important to find out how the difference in the aging dynamics arising from the different localization mechanisms are affected by the

presence of activated processes.

Finally, we have shown that a good agreement is found between experimental and numerical data, also in the aging dynamic.

Acknowledgments

We acknowledge support from MIUR COFIN 2002 and FIRB and from INFM Iniziativa Calcolo Parallelo. We

thank W. C. K. Poon and K. N. Pham for useful discussion and for bringing their results to our attention.

-
- [1] P. N. Pusey, in *Liquids, Freezing and Glass Transition*, edited by J. P. Hansen, D. Levesque, and J. Zinn-Justin (North Holland, Amsterdam, 1991), vol. Session LI (1989) of Les Houches Summer Schools of Theoretical Physics, pp. 765-792.
- [2] A. P. Gast, W. Russell, and C. Hall, *J. Colloid Interface Sci.* 96, 1977 (1983).
- [3] E. Meijer and D. Frenkel, *Phys. Rev. Lett.* 67, 1110 (1991).
- [4] V. Anderson and H. Lekkerkerker, *Nature* 416, 811 (2002).
- [5] F. Sciortino, *Nature Materials* 1, 145 (2002).
- [6] In fact the repulsive glass should be named more correctly "hard-sphere" glass, since this is the real nature of the repulsion in the system we shall study.
- [7] W. Gotze, in *Liquids, Freezing and Glass Transition*, edited by J. P. Hansen, D. Levesque, and J. Zinn-Justin (North Holland, Amsterdam, 1991), vol. Session LI (1989) of Les Houches Summer Schools of Theoretical Physics, pp. 287-503.
- [8] L. Fabbian, W. Gotze, F. Sciortino, P. Tartaglia, and F. Thiery, *Phys. Rev. E* 59, R1347 (1999).
- [9] J. Bergenholz and M. Fuchs, *Phys. Rev. E* 59, 5706 (1999).
- [10] K. Dawson, G. Fo, M. Fuchs, W. Gotze, F. Sciortino, M. Sperl, P. Tartaglia, T. Voigtman, and E. Zaccarelli, *Phys. Rev. E* 63, 011401 (2001).
- [11] G. Fo, G. D. McCullagh, A. Lawlor, E. Zaccarelli, K. A. Dawson, F. Sciortino, P. Tartaglia, D. Pini, and G. Stell, *Phys. Rev. E* 65, 031407 (2002).
- [12] W. Gotze and M. Sperl, *J. Phys.: Cond. Mat.* 15, S869 (2003).
- [13] A. M. Puertas, M. Fuchs, and M. E. Cates, *Phys. Rev. Lett.* 88, 098301 (2002).
- [14] G. Fo, K. A. Dawson, S. V. Buldyrev, F. Sciortino, E. Zaccarelli, and P. Tartaglia, *Phys. Rev. E* 65, 050802(R) (2002).
- [15] E. Zaccarelli, G. Fo, K. A. Dawson, S. V. Buldyrev, F. Sciortino, and P. Tartaglia, *Phys. Rev. E* 66, 041402 (2002).
- [16] A. M. Puertas, M. Fuchs, and M. E. Cates, *Phys. Rev. E* 67, 031406 (2003).
- [17] F. Mallamace, P. Gambadauro, N. Micali, P. Tartaglia, C. Liao, and S.-H. Chen, *Phys. Rev. Lett.* 84, 5431 (2000).
- [18] K. N. Pham, A. M. Puertas, J. Bergenholz, S. U. Egelhaaf, A. Mousa, P. N. Pusey, A. B. Schofield, M. E. Cates, M. Fuchs, and W. C. K. Poon, *Science* 296, 104 (2002).
- [19] T. Eckert and E. Bartsch, *Phys. Rev. Lett.* 89, 125701 (2002).
- [20] S.-H. Chen, W.-R. Chen, and F. Mallamace, *Science* 300, 619 (2003).
- [21] W.-R. Chen, F. Mallamace, C. J. Glinka, E. Fratini, and S.-H. Chen, *Phys. Rev. E* 68, 041402 (2003).
- [22] T. Eckert and E. Bartsch, *Faraday Discuss.* 123, 51 (2003).
- [23] F. Sciortino, P. Tartaglia, and E. Zaccarelli (2003), to be published in *Phys. Rev. Lett.*, cond-mat/0304192.
- [24] E. Zaccarelli, G. Fo, F. Sciortino, and P. Tartaglia, *Phys. Rev. Lett.* 91, 108301 (2003).
- [25] W. Kob and J.-L. Barrat, *Phys. Rev. Lett.* 78, 4581 (1997).
- [26] F. Sciortino and P. Tartaglia, *J. Phys.: Condens. Matter* 13, 9127 (2001), and references therein.
- [27] K. N. Pham, S. U. Egelhaaf, P. N. Pusey, and W. C. K. Poon (2003), to be published, cond-mat/0308250.
- [28] D. C. Rapaport, *The art of computer simulations* (Cambridge Univ Press, London, 1997), 2nd ed.
- [29] L. F. Cugliandolo and J. Kurchan, *Phys. Rev. Lett.* 71 (1993).
- [30] G. Parisi, *J. Phys. A: Math. Gen.* 30, 8523 (1997).
- [31] A. Latz, *J. Phys.: Condens. Matter* 12, 6353 (2000).
- [32] F. Sciortino and P. Tartaglia, *Phys. Rev. Lett.* 86, 107 (2001).
- [33] P. De Groot, F. Sciortino, P. Tartaglia, E. Zaccarelli, and K. Dawson, *Physica A* 307, 15 (2002).
- [34] E. Zaccarelli, G. Fo, K. A. Dawson, S. V. Buldyrev, F. Sciortino, and P. Tartaglia, *J. Phys.: Condens. Matter* 16, S367 (2003).
- [35] G. Fo, W. Gotze, F. Sciortino, P. Tartaglia, and T. Voigtman (2003), to be published in *Phys. Rev. E*, cond-mat/0309007.
- [36] L. F. Cugliandolo, lecture notes, Les Houches, July 2002, cond-mat/0210312.
- [37] N. W. Ashcroft and N. D. Mermin, *Solid state physics* (International Thomson Publishing, Washington, DC, 1976).
- [38] E. Zaccarelli, G. Fo, P. D. Groot, F. Sciortino, P. Tartaglia, and K. A. Dawson, *J. Phys.: Condens. Matter* 14, 2413 (2002).

Figures

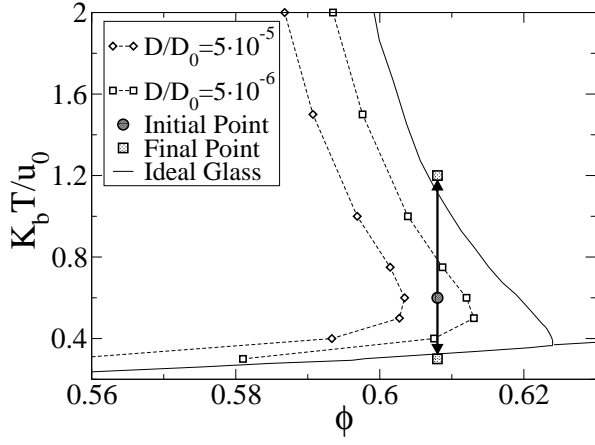


FIG. 1: Square Well iso-diffusivity curves (i.e. the locus of points in the ϕ - T plane where the normalized diffusion coefficient \bar{D} is constant) for three different values of D/D_0 ($D_0 = \bar{D}_b(T_m)$ data from Ref.[38]). The extrapolated ideal glass line is also reported (data from Ref.[23]). Equilibrium starting configurations at $\phi = 0.608$ and $T_i = 0.6$ (red circle) are instantaneously quenched at $t = 0$ to $T_f = 0.3$ and $T_f = 1.2$ (plus).

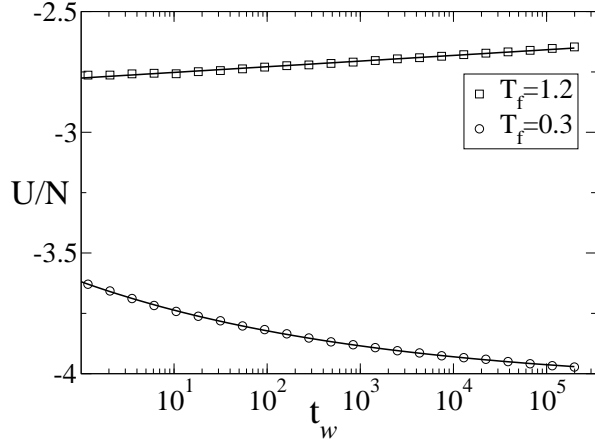


FIG. 2: Average potential energy U after the quench as function of the time t_w elapsed from the quench. The symbols are the simulation data and the continuous lines are the fits. Data for $t_w < 1$ are not shown since the kinetic energy has not yet equilibrated to the final value. For $T_f = 1.2$ the fit is $U/N = -2.77 + 0.01 \ln(t_w)$ while for $T_f = 0.3$ we obtain $U/N = -4.05 + 0.43 t_w^{0.14}$.

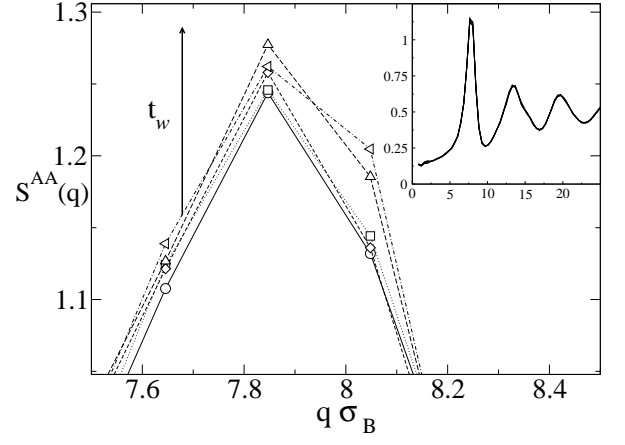


FIG. 3: First peak of the static structure factor at different waiting time t_w , 10^1 (circles), 10^2 (squares), 10^3 (diamonds), 10^4 (triangles up) and 10^5 (triangles left). The quench is at $T_f = 1.2$. For long t_w there is slow growth of the peaks of the structure factors. In the inset structure factors for the same t_w are displayed.

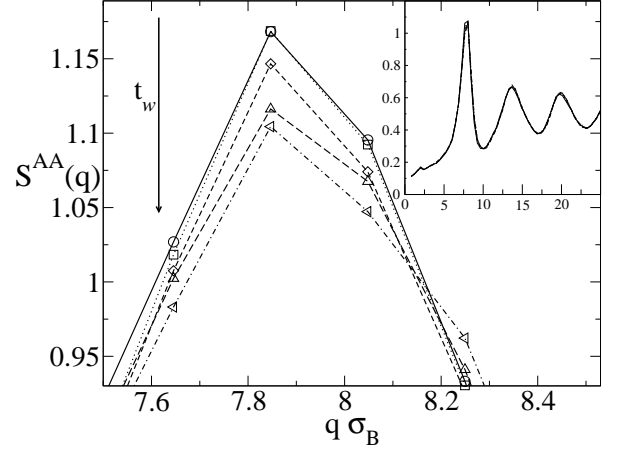


FIG. 4: Same as Fig. 3 for $T_f = 0.3$.

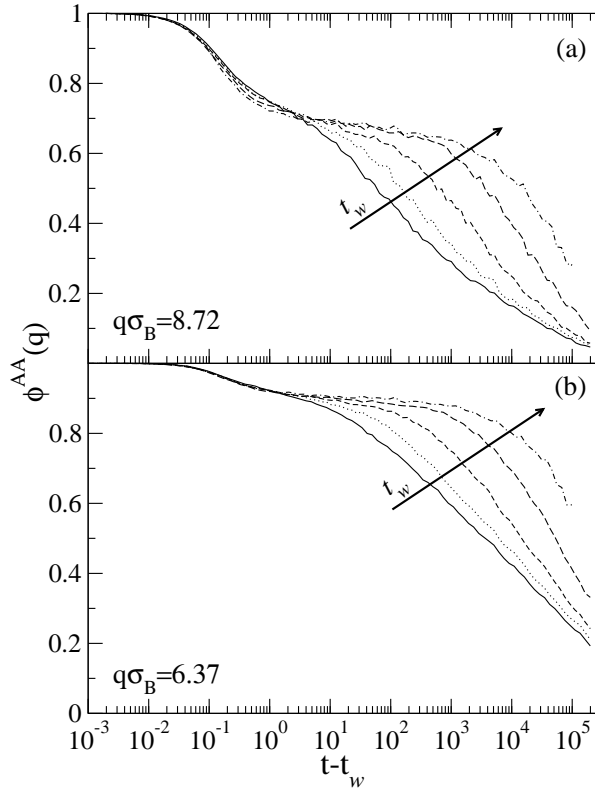


FIG. 5: (a) Density-density correlation function $\phi_{AA}(q; t_w; t - t_w)$ after a quench at $T_f = 1.2$ for $q \sigma_B = 8.72$. From right to left, longer and longer relaxation time, $t_w = 10^1$ (continuous line), 10^2 (dotted line), 10^3 (short dashed line), 10^4 (long dashed line), 10^5 (dot dashed line). (b): same results but for $q \sigma_B = 6.37$

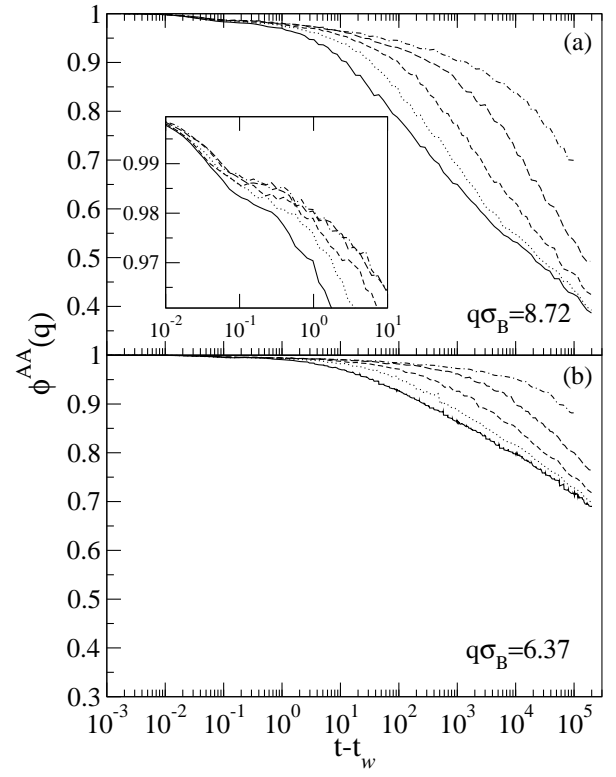


FIG. 6: Same as Fig. 5 but for the quench at $T_f = 0.3$. In the inset in (a), an enlargement of the plateau area is shown (see text for details).

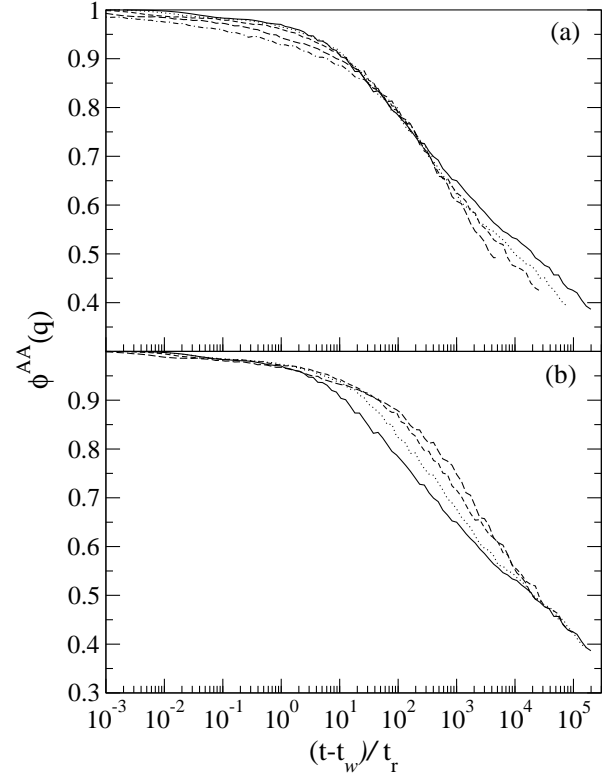


FIG. 7: Scaling of the density-density correlation functions for $T_f = 0.3$. The waiting times are $t_w = 10^1$ (continuous line), 10^2 (dotted line), 10^3 (short dashed line), 10^4 (long dashed line), 10^5 (dot dashed line).
 (a) best scaling for the region where $0.7 < q < 0.9$.
 (b) best scaling for the region where $0.35 < q < 0.5$.

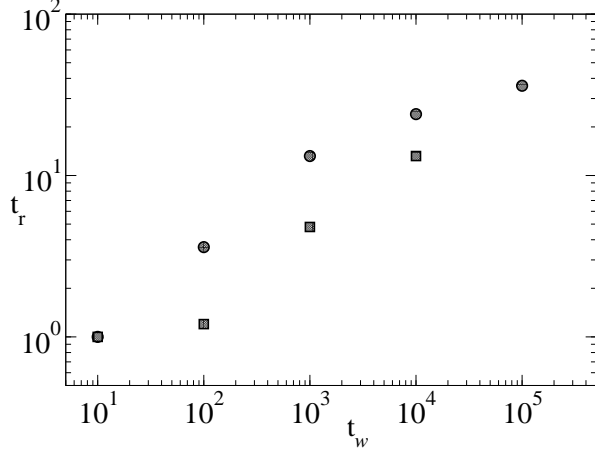


FIG. 8: Scaling coefficient used to obtain the scaling in Fig. 7a-b. The circle are the scaling coefficient for the case in Fig. 7a, the square for 7b.

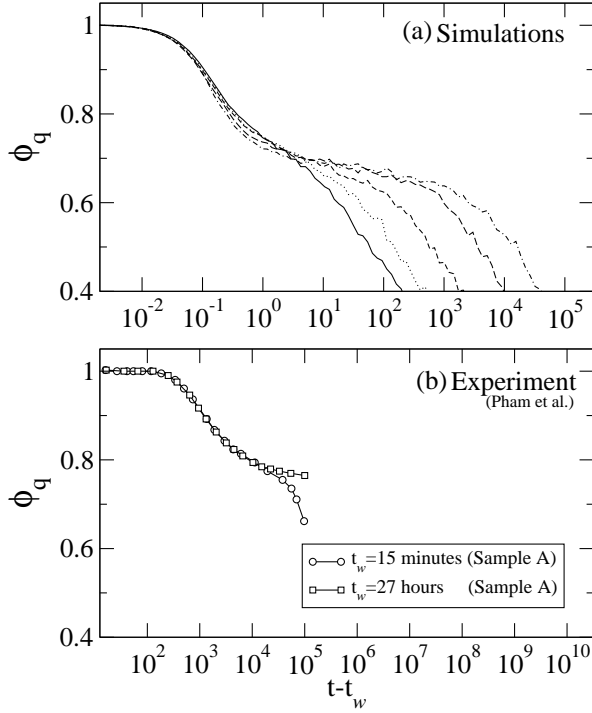


FIG. 9: Upper panel: total density-density correlation functions for $q_{R_A} = 2.93$ at different waiting times for $T_f = 1.2$. From right to left, longer and longer relaxation time, $t_w = 10^1; 10^2; 10^3; 10^4; 10^5$. Lower Panel: Experimental data reproduced from [27]. The unit of time are in seconds but time has been rescaled by the relative viscosity of the solvent and the wave vector.

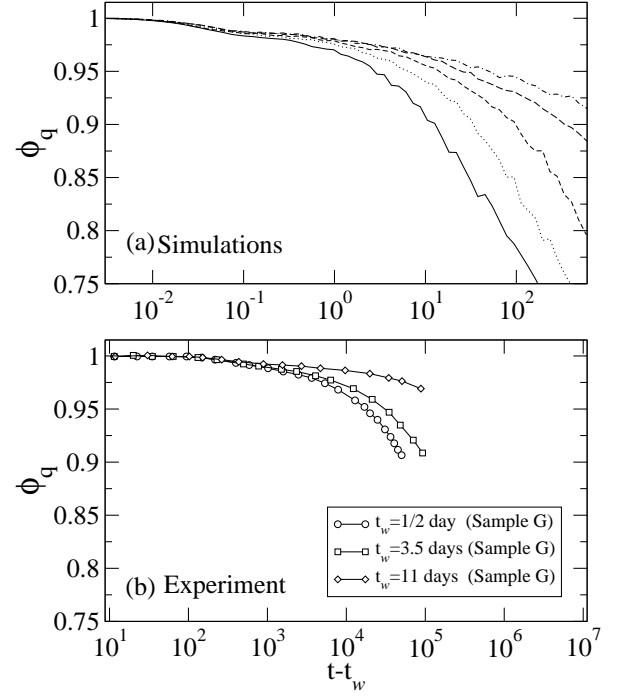


FIG. 10: Upper panel: Same as in Fig. 9 for $T_f = 0.3$. Lower panel: Again experimental data are taken from [27].

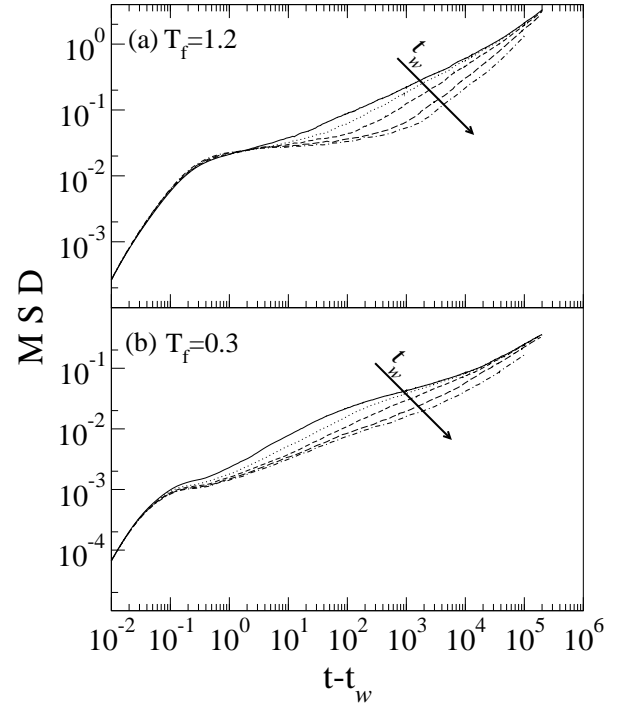


FIG. 11: (a) Mean square displacement (MSD) for the quench at $T_f = 1.2$ for increasing waiting times $t_w = 10^1$ (continuous line), 10^2 (dotted line), 10^3 (short dashed line), 10^4 (long dashed line), 10^5 (dot dashed line).
 (b) As in (a) for $T_f = 0.3$